DYNAMIC RESPONSE ANALYSIS AND OUTPUT VOLTAGE CONTROL OF CURRENT-FED FULL-BRIDGE DC–DC CONVERTER USING ARTIFICIAL BEE COLONY OPTIMIZED PI CONTROLLER

V.Delbin Jelaja
Department of Electrical Engineering, Anna University, Chennai, India

M.Rajaram
Vice Chancellor, Anna University, Chennai, India

Abstract*: In this article, an Artificial Bee Colony algorithm is proposed to determine the gain parameters of the PI controller and to improve the performance of the current-fed full-bridge DC–DC converter. To investigate the performance of the proposed algorithm the conventional PI controller is also incorporated into the system. Simulations are done for different input voltages and load conditions. In the simulation of the proposed converter the settling time, low frequency gain and steady state error of the system in case of load variations are analyzed. A converter prototype of 300 W is also developed and tested with the implemented converter to observe the performance of the system. Finally the analysis and complete controller design show that the ABC-PI-controlled converter has superior performance, satisfactory and stable transient response with continued safe operation.*

Keywords*: DC–DC converter, PI controller, Artificial Bee Colony, Small Signal Modeling, Dynamic response*

1. Introduction

As the world's power demand increases, energy saving and conservation have become imperative. Lots of research have been carried out to provide energy in a clean and efficient way. Renewable energy sources such as PV, wind and fuel cells are the most promising ways for clean electric power generation. But these distributed energy sources have brought in their wake issues like system stability, reliability and power quality. These energy sources are integrated with an energy storage system for backup power to form a distributed generation system for long term sustainability. High frequency isolated DC–DC converter topologies [1–5] are more suitable for this application, because they translates the low fuel cell stack voltage to higher than the peak utility grid. The input to these converters is often an unregulated and rectified line voltage, which will fluctuate due to changes in line voltage magnitude. The aim of feedback control is to convert the unregulated DC input into a regulated DC output at a desired level and to keep the DC output at this level if there are any variations of the load. Various control strategies [6, 7] are used to control the output voltage of DC–DC converters such as PI control, Pole placement and feedback loop etc. that are used for different applications of power system components. A powerful method to control the output voltage is PI control method. But, in the PI control method choosing the parameters is hard because DC–DC converters contain parasitic components and changes in input voltage and output load. Therefore, PI controller parameters must be designed effectively to obtain robust transient response. Initially, Ziegler Nichols and various other classical methods were used to perform this operation. But, these classical methods have certain disadvantages such as complex mathematical computations, huge overshoots and unsatisfactory gain and phase margins.

In recent years, artificial intelligence optimization techniques [8–10] have been used frequently to design the PI controller parameters. Algorithms such as Particle Swarm Optimization [11–14], Fuzzy logic, Bacterial foraging optimization or genetic algorithm [15, 16] have been implemented to determine the PI controller parameters. However, they too have certain limitations such as the difficulty of creating fuzzy rules in fuzzy logic, premature convergence and long computation time. ABC algorithm was first proposed by Karaboga has a simple structure, less control parameters and gives strong solutions to different fitness functions when compared to other optimization algorithms like PSO and GA. But in this article ABC optimization algorithm is used to determine the PI controller control parameters for controlling the DC–DC converters.

An active clamp current-fed full-bridge isolated zero-voltage-switching (ZVS) topology has been analyzed and discussed in [17]–[21]. But, the main focus of the article is ABC optimization algorithm is used for improving the response of active clamped current-fed full-bridge DC–DC converter for high voltage applications. The circuit diagram of the proposed converter is shown in Fig. 1.

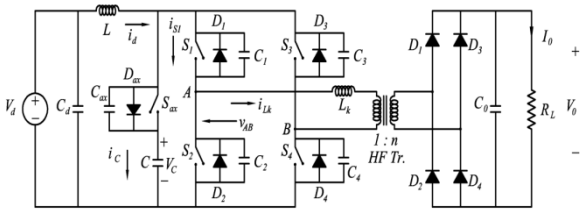

Fig 1. Circuit diagram of the proposed converter

The objectives are achieved and outlined in this article are as follows. The small signal modeling of the converter and its transfer functions are derived in section II. The ABC-PI-based control of the proposed converter is presented in section III. The closed controller design using two-loop average current control method is presented in section IV. The frequency response curves are plotted to verify the stability of the current controller and the complete system. Simulation of the proposed converter using ABC optimization algorithm is presented in section V. Experimental results obtained by testing a 300 W converter prototype is demonstrated to show the transient response and converter performance for step change in load at different input voltage and load conditions.

2. Small-Signal Analysis

In this section, small signal analysis and transfer functions of the proposed converter are discussed. Steady state operating waveforms are shown in Fig 2. The circuit undergoes five different intervals of operation over a half switching period. The state variables meant for small signal analysis of the converter are defined as follows

(i) The current through the input inductor (i_d)
(ii) The current through the transformer leakage inductor (i_{LK})
(iii) The voltage across the auxiliary capacitor (V_c)
(iv) Output Voltage (V_0)
(v) Duty Cycle (d)

Since the current through the transformer leakage inductance is discontinuous, the average value of rate change of current over one complete cycle is zero and the average state equation is

$$L_K\left\langle\frac{di_{LK}}{dt}\right\rangle=0 \tag{1}$$

Therefore, the above state variable i_{LK} is omitted for further analysis.

The duty cycle of the main switches (including conduction of the anti-parallel diode) is defined as

$$d_{sw1}=d_{sw4}=d_1+d_4+d_5+d_6+d_7+d_8+d_9+d_{10} \tag{2}$$

$$d_{sw2}=d_{sw3}=d_1+d_2+d_3+d_4+d_5+d_6+d_9+d_{10} \tag{3}$$

$$d_{swax}=d_2+d_3+d_7+d_8 \tag{4}$$

The turn-off durations of the main switches is given by

$$d'_{sw1}=d'_{sw4}=(1-d)=d_2+d_3 \tag{5}$$

$$d'_{sw2}=d'_{sw3}=(1-d)=d_7+d_8 \tag{6}$$

The discharging duration of the transformer leakage inductor is as follows

$$d''=d_4+d_5=d_9+d_{10} \tag{7}$$

The average value of state equations over half switching period is defined as

$$L\left\langle\frac{di_d}{dt}\right\rangle=v_d-2(1-d)v_c \tag{8}$$

$$C\left\langle\frac{dv_c}{dt}\right\rangle=2\left(i_d(1-d)-i_{LK}(1-d)\right) \tag{9}$$

$$C_0\left\langle\frac{dv_0}{dt}\right\rangle=i_{LK,avg}-\frac{v_0}{R_L} \tag{10}$$

The averaged rectified current is as given below

$$i_{LK,avg}=\frac{2i_d}{n}(d_2+d_3+d_4+d_5) \tag{11}$$

Application of volt-sec balance across the transformer leakage inductor during the positive half cycle gives

$$\left[\frac{v_d}{2(1-D)}-\frac{v_0}{n}\right](d_2+d_3)=\frac{v_0}{n}(d_4+d_5) \tag{12}$$

Where, $V_c=\dfrac{v_d}{2(1-D)}$

$$\left[V_c-\frac{v_0}{n}\right](d_2+d_3)=\frac{v_0}{n}(d_4+d_5) \tag{13}$$

The above equations are simplified in terms of duty cycles and result in the following equations

$$L_K\frac{di_{LK}}{dt}=\left(V_c-\frac{v_0}{n}\right)(d_2+d_3) \tag{14}$$

$$i_{LK}=\frac{T_s}{L_K}\left(V_d-\frac{v_0}{n}\right)(1-d) \tag{15}$$

$$C\left\langle\frac{dv_c}{dt}\right\rangle=2i_d(1-d)-\frac{2T_s}{L_K}\left(V_c-\frac{v_0}{n}\right)(1-d)^2. \tag{16}$$

$$C_0\left\langle\frac{dv_0}{dt}\right\rangle=\frac{2i_d}{n}(1-d+d'')-\frac{v_0}{R_L} \tag{17}$$

Perturbation around the steady state value of the state variables and other quantities is given by

$$i_d=I_d+\hat{i}_d,\quad v_c=V_c+\hat{v}_c,\quad v_d=V_d+\hat{v}_d$$

$$v_0=V_0+\hat{v}_0,\quad d=D+\hat{d}$$

Comparison of AC quantities in the above equations while neglecting second order terms, results in the following AC equations

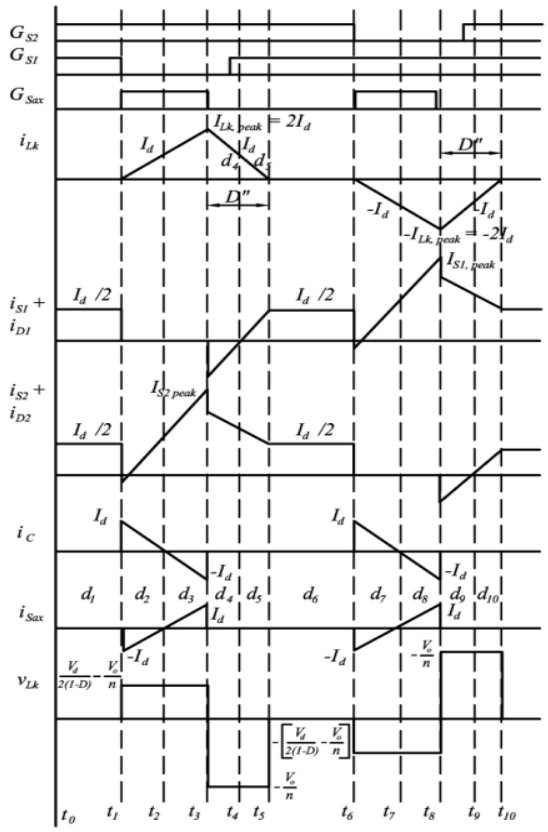

Fig 2. Steady state operating waveforms of the proposed converter

$$C\frac{d\hat{v}_c}{dt} = 2(1-D)\hat{i}_d - 2I_d\hat{d} - \frac{T_s}{L_k}\left(\hat{v}_c - \frac{\hat{v}_0}{n}\right)(1-D)^2 + 2\frac{T_s}{L_k}\left(V_c - \frac{V_0}{n}\right)(1-D)\hat{d}. \quad (18)$$

$$L\frac{d\hat{i}_d}{dt} = \hat{v}_d - 2(1-D)\hat{v}_c + 2V_c\hat{d} \quad (19)$$

$$C_0\frac{d\hat{v}_0}{dt} = 2\frac{\hat{i}_d}{n}(1-D+D'') - 2\frac{I_d}{n}\hat{d} + 2\frac{I_d}{n}\hat{d}'' - \frac{\hat{v}_0}{R_L} \quad (20)$$

$$\left(\hat{v}_c - \frac{\hat{v}_0}{n}\right)(1-D) - \left(V_c - \frac{V_0}{n}\right)\hat{d} = \frac{\hat{v}_0}{n}D'' + \frac{V_0}{n}\hat{d}'' \quad (21)$$

Laplace transform of the above equation and the writing of it in matrix form is as Follows

$$\begin{bmatrix}\hat{i}_d(s)\\ \hat{v}_c(s)\\ \hat{v}_0(s)\end{bmatrix} = \begin{bmatrix} sL & 2(1-D) & 0 \\ -2(1-D) & sC + \frac{(1-D)^2}{f_s L_k} & \frac{-(1-D)^2}{nL_k f_s} \\ -2\left(\frac{1-D-D''}{n}\right) & -2\frac{I_d}{V_0}(1-D) & sC_0 + \frac{1}{R_L} + \frac{2I_d}{nv_0}(1-D+D'') \end{bmatrix}\begin{bmatrix}c_1\\ c_2\\ c_3\end{bmatrix}\hat{d}(s) + \begin{bmatrix}1\\ 0\\ 0\end{bmatrix}\hat{v}_d(s) \quad (22)$$

Equation (22) represents the small signal model of the proposed converter in matrix form. This model can also be used for the design of the closed-loop control system of the converter. The transfer function of the system can also be calculated by using this model.

3. ABC-PI-Based Control of the Proposed Converter

Artificial Bee Colony (ABC) algorithm is one of well-established swarm intelligence-based stochastic optimization algorithms, which draws its inspiration from the foraging and communication mode of bees. In ABC algorithm the artificial bees are categorized into three groups, namely onlooker bees, employed bees and scouts. The sum of the employed bees and the onlooker bees is the total number of bees in a colony. The role of an employed bee is to hover over a potential food source and to collect and store information regarding a food source in its memory. The onlooker bee gets information regarding food sources through the dances of employed bees. One to one selection is made by onlookers for choosing an employed bee and the onlookers try to exploit the food source to gather the nectar.

For every food source, there is only one employed bee and the employed bee of an abandoned food source becomes a scout. This scout helps in exploring sites for more potential food sources. The quality of the optimized solution is based mainly on the profitability of the food source. In ABC algorithm, the position of a food source represents a possible solution to be optimized.

The proposed DC–DC converter designed using ABC-tuned PI controller is shown in Fig. 3. The output voltage of the proposed converter should be kept at a stable value by using ABC-PI-controlled structure. The control model consists of two loops, the inner current control loop and the outer voltage control loop. The outer voltage control loop regulates the output voltage by generating the reference inductor current for the current control loop. The ABC-tuned PI controller computes the control variable value by using its gain parameters and error value. The controller output is compared with the modulator to obtain the gating signals of the devices. This process can be modeled mathematically

$$e(t) = V_0 - V_{ref} \quad (23)$$

$$u(t) = k_p e(t) + k_i \int_0^t e(t)dt \quad (24)$$

Where, $e(t)$ – The error
V_{ref} – Reference voltage
V_o – Output voltage

In the ABC-tuned PI controller, the control parameters are defined optimally. ABC algorithm is used to define the PI parameters $\lfloor k_{p1}, k_{i1}, k_{p2}, k_{i2} \rfloor$ optimally. The main steps of the algorithm are as follows.

Step 1: Get the input data. The input data are limits of PI controller Parameters.

Step 2: Initialize ABC parameters like colony dimension, maximum cycle number, number of variables and limit parameters.

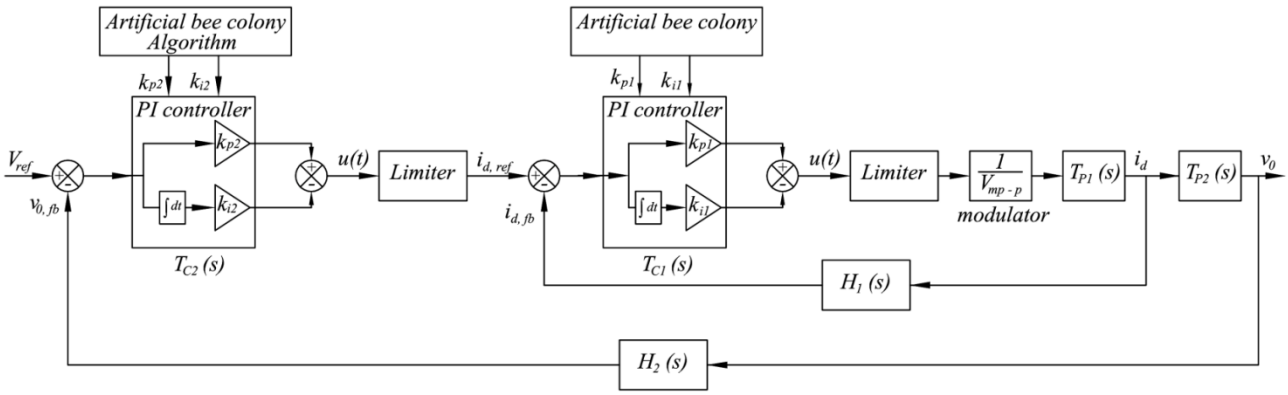

Fig 3. Complete ABC-PI control model of the proposed converter

Colony dimension = 50
Maximum number of foraging cycle = 100
No of variables = 4
PI controller limits:

$k_{p1} = [1\ 2.5]$ $k_{i1} = [5000\ 6000]$

$k_{p2} = [75\ 150]$ $k_{i2} = [8500\ 9000]$

Step 3: Initialization of population
A set of initial population with N solutions are randomly produced by the following equation

$$x_{ij} = x_j^{\min} + \left(x_j^{\max} - x_j^{\min}\right) * rand(0,1). \quad (25)$$

Here each solution of x_i represented by D-dimensional vector corresponded to number of PI parameters to be optimized. $x \in [k_{p1}, k_{i1}, k_{p2}, k_{i2}]$

Step 4: Evaluate fitness of the population
Fitness values obtained from the fitness function belonging to each solution is evaluated at this step. The fitness function for the design of DC–DC converters is described as follows:

$$Minimize,\ fit_k = \sum_{t=1}^{n} e^2(t) \quad (26)$$

where, $e(t)$ is the error value defined in eqn. (23) and n is the maximum iteration number for determined PI parameters at one cycle of ABC algorithm.

Step 5: Set the cycle counter to 1

Step 6: For each employed bee, a new source is produced by the following equation.

$$v_{ij,new} = x_{ij} + \beta_{ij}\left(x_{ij} - x_{kj}\right) \quad (27)$$

where, β_{ij} is a uniformly distributed real random number within the range [–1, 1]

Step 7: New solution v_{ij} is compared with the old solution x_{ij} and the best one is exploited by the employed bee.

Step 8: Each onlooker bee prefers a food source site with the probability calculated by the following equation

$$P_i = \frac{fit_i}{\sum_{j=1}^{FS} fit_j} \quad (28)$$

where, fit_i is the fitness value of the i^{th} food source, if the problem used here is a minimization problem, then fitness is evaluated according to the following equation:

$$fit_i = \frac{1}{1 + X(J)} \quad (29)$$

Where X(J) represents the objective function to be minimized, as shown in eqn. (26)

Step 9: Scout bee explores new food sources. If a food source has been exhausted after a number of trials it will be abandoned. The scout will explore a new food source randomly according to the equation

$$x_{ij,new} = x_j^{\min} + \left(x_j^{\max} - x_j^{\min}\right) * rand(0,1) \quad (30)$$

Step 10: Memorize the best solution obtained so far

Step 11: Increase the cycle counter

4. Controller Design: Two-loop Average Current Control Method

4.1 Control-to-output voltage transfer function

The design of closed-loop controller using two-loop average current control method is explained in this section. For voltage control loop, the transfer function of the control to output of the overall system can be calculated by setting $\hat{v}_d(s) = 0$ in the small signal model of the proposed converter and it is given by

$$\frac{\hat{v}_0(s)}{\hat{d}(s)} = \frac{a_0 s^2 + a_1 s + a_2}{b_0 s^3 + b_1 s^2 + b_2 s + b_3} \quad (31)$$

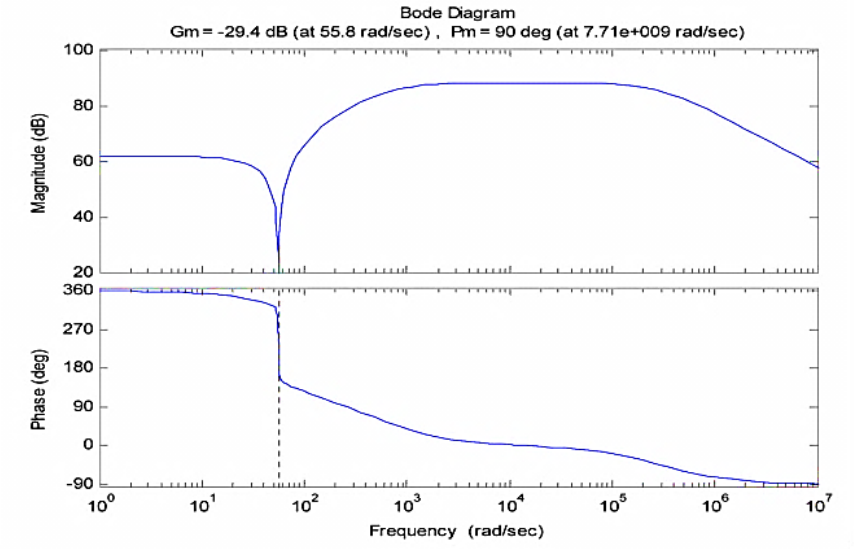

Fig 4. Frequency response of control to output voltage transfer function of the system without controller

The numerator and denominator coefficients of the control to output voltage transfer function are given in appendix A

$$\frac{\hat{v}_0(s)}{\hat{d}(s)} = \frac{7.713\times10^9 s^2 - 6.717\times10^9 s + 2.3522\times10^{13}}{s^3 + 3.0305\times10^5 s^2 + 2.275\times10^8 s + 1.904\times10^{10}} \quad (32)$$

The bode response of the control to output voltage transfer function of the system without controller is shown in Fig. 4. From the bode response the gain margin of the system is negative, which makes the system unstable for small disturbances in source voltage (or) load. For a stable and continuous operation of the converter, design it with a PI controller and an ABC algorithm is used to define the PI controller parameters optimally to obtain an effective (or) robust transient response

4.1.1 Design of current control loop

To design a current controller loop, the first step is to consider the stability and response criteria. Here, the inductor current is fed back to the closed-loop controller with the gain of $H_1(s)$. The transfer function of inductor current to the duty ratio can be obtained from eqn. (22).

$$T_{p1}(s) = \frac{\hat{i}_d(s)}{\hat{d}(s)} = \frac{a_0 s^2 + a_1 s + a_2}{b_0 s^3 + b_1 s^2 + b_2 s + b_3} \quad (33)$$

The numerator and denominator coefficients of the inner current controller loop are given in appendix B

PI Controller design:

A PI controller is designed to increase the low frequency gain and to reduce the steady state error between the actual and desired values of inductor currents

$$T_{C1}(s) = k_{p1} + \frac{K_{i1}}{s}. \quad (34)$$

Modulator design:

The voltage signal at the output of the current controller is converted from analog to digital and used as a duty ratio to control the main switch as well as auxiliary switches. Considering the gain of the analog to digital converter and neglecting the conversion delay in the same and subsequent digital process, the overall modulator gain is given as

$$T_{m1}(s) = \frac{1}{13.2} \quad (35)$$

The maximum current through the boost inductor is set at 25 A and the corresponding voltage as 2.5 V, which is set as the limit of the voltage controller. This gives the feedback gain of the current controller

$$H_1(s) = \frac{1}{10}. \quad (36)$$

Hence, the overall transfer function of the current control loop is given by,

$$T_{OL1}(s) = T_{c1}(s)T_{m1}(s)H_1(s)T_{p1}(s) \quad (37)$$

$$T_{OL1}(s) = \frac{K_{p1}(s + K_{i1}/K_{p1})\times(5\times10^5 s^2 + 1.52\times10^{11} s + 3.598\times10^{12})}{10\times13.2S(S^3 + 3.03\times10^5 S^2 + 2.275\times10^8 S + 1.904\times10^{10})} \quad (38)$$

The bode plot of the current control loop with PI controller and ABC-tuned PI controller response for input voltage = 22 V and R_L =400Ω are obtained in Fig. 5. From this figure, it can be easily seen that, general PI controller shows a PM = 60°at 6.07 krad/sec and ABC-tuned PI Controller shows a PM = 72.1° at 8.06 krad/sec. From this fig, by using the ABC algorithm, the phase margin of the system and low frequency gain are improved.

4.1.2 Design of voltage control loop

Outer voltage control loop regulates the output voltage by setting inductor current as reference. The inner current control loop has faster dynamics as compared to outer voltage control loop. Hence, the current loop dynamics is not taken into consideration while designing the voltage controller. To design the voltage controller, the inductor current to output voltage transfer function is obtained as

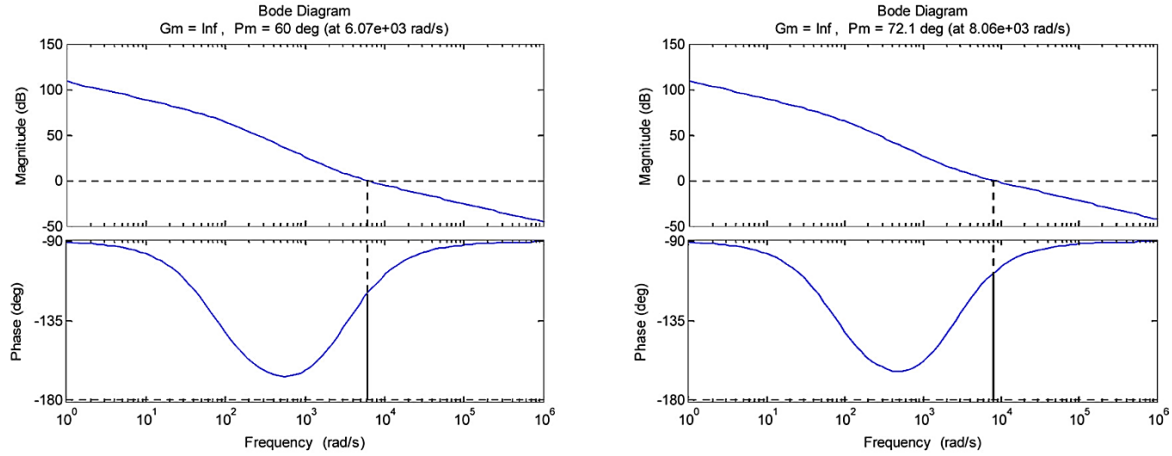

(a) (b)

Fig 5. Bode plot of Current controller loop with V_d = 22 V at R_L = 400 Ω (a) With PI Controller (b) With ABC-tuned PI controller

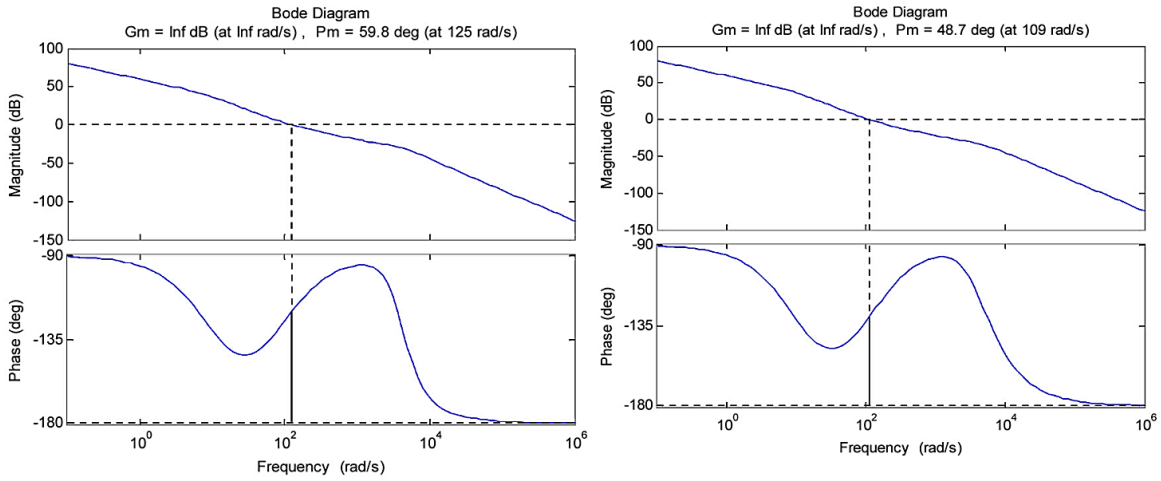

(a) (b)

Fig 6 Bode plot of overall system with V_d = 22 V at R_L = 400 Ω (a) With PI controller (b) With ABC-tuned PI controller

$$T_{p2}(s) = \frac{\hat{v}_0(s)}{\hat{i}_d(s)} = \frac{2(1-D+D'')}{nC_0 s + n/R_L} \tag{39}$$

By calculating the voltage feedback gain the reference voltage is set at 1.75 V corresponding to the output voltage of 350 V.

$$H_2(s) = \frac{1}{200} \tag{40}$$

The transfer function of PI controller for voltage loop is given by

$$T_{c2}(s) = \frac{k_{p2}\left(s + k_{i2}/k_{p2}\right)}{s} \tag{41}$$

For voltage control loop, the open loop transfer function is given by

$$T_{OL2}(s) = T_{c2}(s)T_{p2}(s)H_2(s). \tag{42}$$

The transfer function of the complete system including current and voltage control loop can be written as

$$T_{OL}(s) = \left[\frac{T_{OL1}(s)}{1+T_{OL1}(s)}\right]T_{OL2}(s). \tag{43}$$

The stability of the control system and the controller design are verified by plotting the frequency response curves of the overall system for input voltage = 22 V and R_L = 400 Ω shown in Fig. 6. From this fig, it can be easily seen that a PI controller shows a PM = 59.8°, at 125

rad/sec and ABC-tuned PI controller shows a PM = 48.7 at 109 rad/sec. From this fig, it is seen that ABC-tuned PI algorithm has a high low-frequency- gain as compared to a conventional PI Controller that helps to achieve low or negligible steady – state error. Table 3 shows the values of GM and PM at corresponding crossover frequencies fordifferent input voltages and load conditions. This table also shows how ABC-tuned PI controller results are better as compared to the conventional PI controller results for the same frequency. Through this system stability over large operating range of input voltage and load is ensured

5. Simulation Results

The performance of the proposed DC–DC converter is investigated by using the simulation of ABC-PI algorithm. In this study, the conventional PI controller is also implemented on the same converter and results obtained there from are compared with ABC-tuned PI algorithm to show the effectiveness of the ABC PI algorithm. ABC parameters used in the simulation are given in Table.1.

Fig. 7 shows the simulated waveforms of ABC –PI algorithm for different input voltage and load conditions. Figs. 7(a) and (b) show the waveforms of V_d = 22 V and V_d = 40 V for R_L = 400 Ω. From the waveforms the settling time of PI controller is 2 sec and the settling time of ABC –PI controller is 1.2 sec. Also, Figs. 7(c) and (d) show the waveforms of V_d = 22 V and V_d = 40 V for R_L = 450 Ω. From the waveforms the settling time of PI controller is 2.3 sec and the settling time of ABC-PI controller is settled below 0.5 sec. Also Figs. 7(e) and (f) show the waveforms of V_d = 22 V and V_d = 40 V for R_L = 500 Ω. From the waveforms the ABC –PI controller is settled below 0.5 sec But PI controller takes a long time to settle. It is clearly seen that the results ABC-tuned PI algorithm produces more robust results to control the DC–DC converter from the point of settling time. It demonstrates the fact that the performance of the converter is stable over a wide operating range.

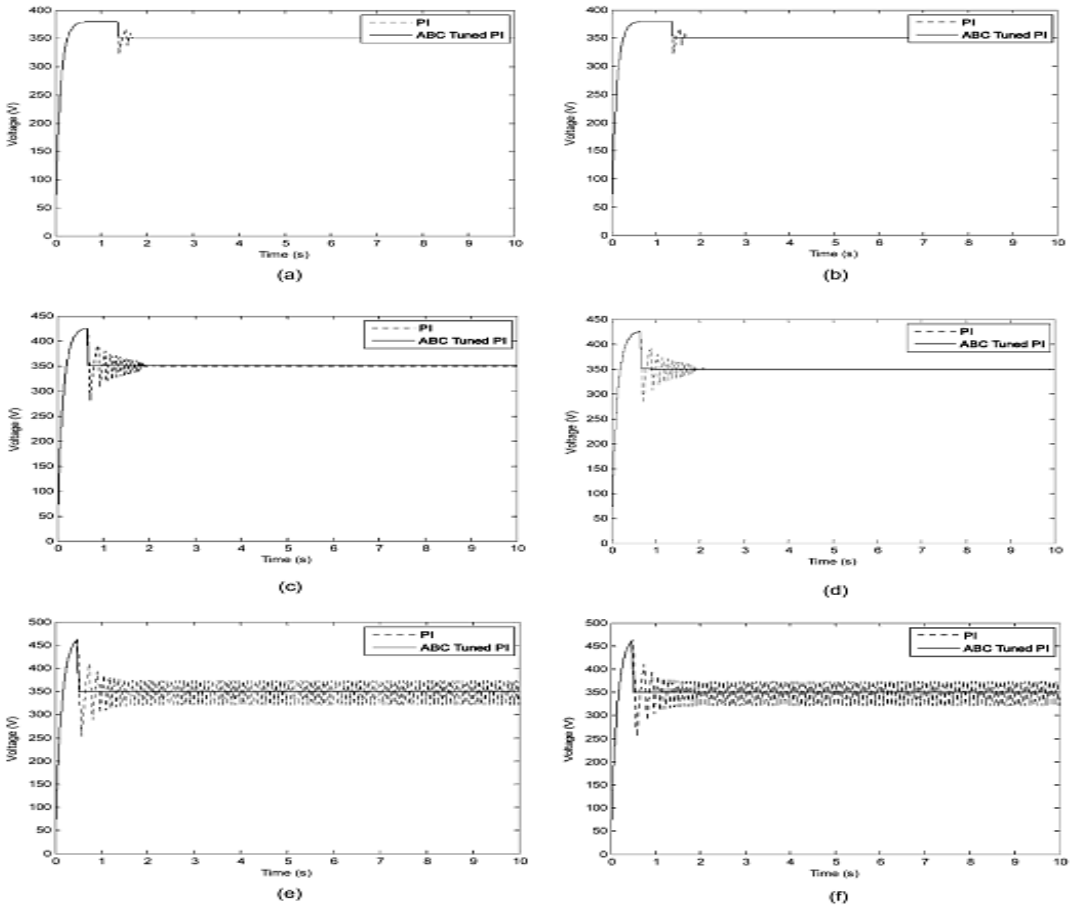

Fig 7. Simulated waveforms of the proposed converter under different load conditions (a) V_d = 22 V, R_L = 400 Ω (b) V_d = 40 V, R_L = 400 Ω (c) V_d = 22 V, R_L = 450 Ω (d) V_d = 40 V, R_L = 450 Ω (e) V_d = 27 V, R_L = 500 Ω (f) V_d= 40 V, R_L = 500 Ω

6. Experimental Results

The complete block diagram of the proposed converter is shown in Fig. 3. The experimental set up of the proposed converter shown in Fig. 8. was built as per the specifications given in Table 2. The LEM sensors LV-25-P and LTS25-NP are used to sense the load voltage and input inductor current and also provide the isolation between the controller and the power circuit. The analog to digital converter is used to convert the analog output of the current controller into digital. The gate signals of the main switches are generated by using synchronized PWM blocks. The complementary gating of the auxiliary switches is generated by using the combinational logic blocks. The performance of the proposed converter is verified by driving the experimental setup of the designed controller for different input voltage and load conditions. Experimental waveforms are shown in Figs. 9–11. Fig. 9 shows experimental waveforms V_o and i_o of a general PI controller. From the fig, it is observed that there is ripple in output voltage. The general PI controller brings the output voltage back to the reference value with a settling time of nearly 30–40 ms.The current waveform also shows spikes in output current. From Figs. 10 (e) and (f) the input inductor current (i_d) and the output load current (i_0) settle at their new steady state values smoothly, because of the automatic adjustment of duty cycle to control the closed-loop controller. From Figs. 10(c) and 11 (c) the voltage across the primary side of the transformer (V_{AB}) does not show any oscillations during the transient period, confirming that the switches do not experience any temporary voltage spike during the change in load, which ensures the safe operation of switches. The waveforms clearly indicate that the output voltage (V_0) remains constant with change in load. The designed controller makes sure that the system is stable and holds well for real time applications. It regulates the output voltage and power with high performance and safe operation.

Table1 ABC Parameters

ABC Parameters	Values
Colony Dimension	50
Maximum Cycle number	100
Number of variables	4
Limit Parameter	100

Table 2 Parameters of the proposed converter

Item	**Symbol**	**Value /Part**
Input voltage	V_d	22-41 V
Power Rating	P_0	300 W
Switching frequency	f_s	50 kHz
Transformer	n	8
Leakage inductance	L_{LK}	0.4 µH
Boost inductor	L	220 µH
Clamp Capacitor	C	3.3 µF
Output capacitor	C_0	270 µF
Output Voltage	V_0	350 V
Load resistance	R_L	400 Ω

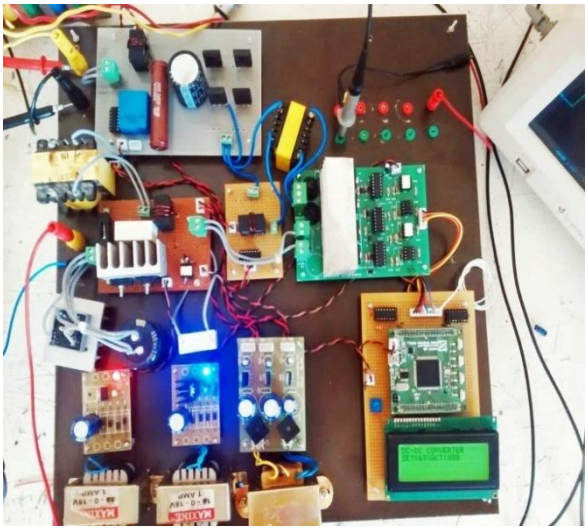

Fig 8. Experimental set up of the proposed converter

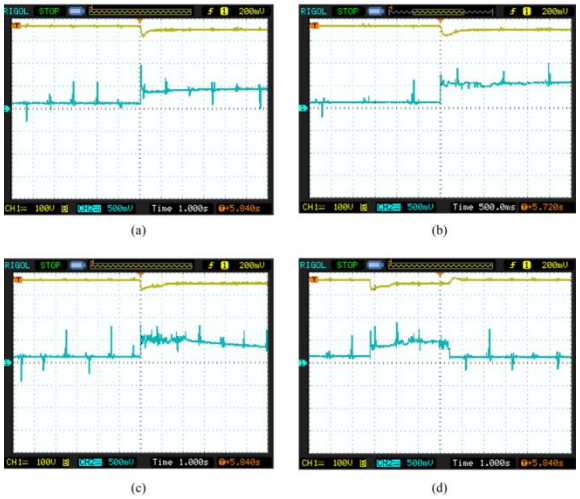

Fig. 9 Experimental waveforms of general PI controller Load Voltage and Load Current on different load condition input V_d = 22 V, at (a) no load, (b) 25% load, (c) 80% load, and (d) full load conditions

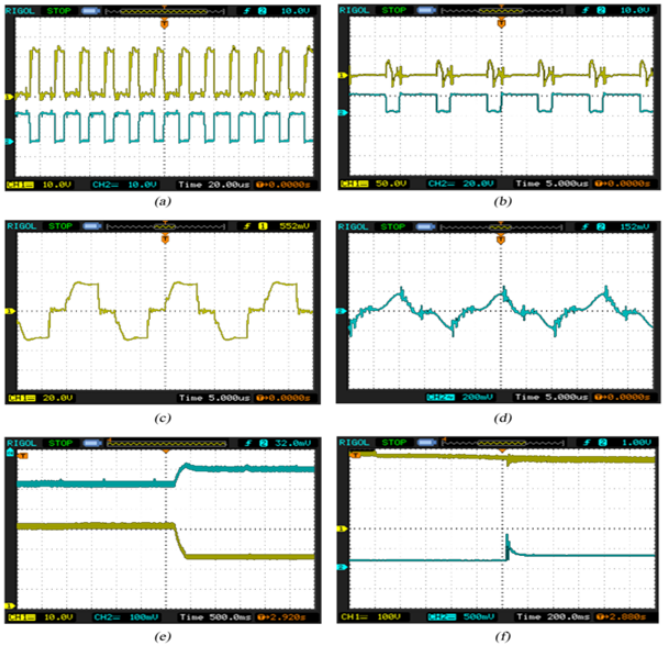

Fig. 10 Experimental Waveforms of Input voltage = 22 V (a) Gate Pulses of main switches (10 V/div) (b) Auxiliary switch voltage (50 V/div) and Gate pulse of auxiliary switch (20 V/div) (c) Voltage across the primary side of the transformer (20 V/div) (d) Current through the primary side of the transformer (12 A/div) (e) Input voltage (20 V/div) and Input current (12 A/div) (f) Output voltage (100 V/div) and output current (1 A/div

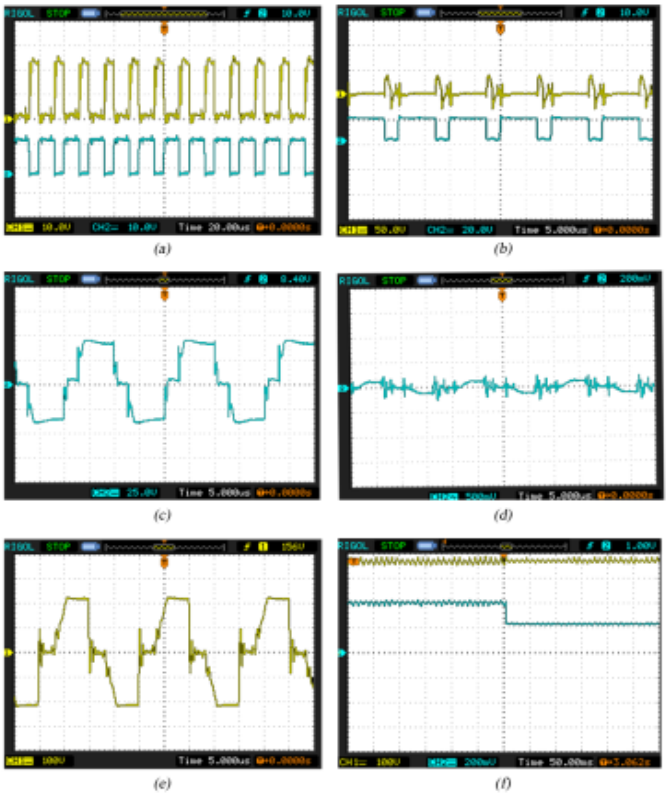

Fig. 11. Experimental Waveforms of Input voltage = 41 V (a) Gate Pulses of main switches (10 V/div) (b) Auxiliary switch voltage (50 V/div) and gate pulses of auxiliary switch (20 V/div) (c) Voltage across the primary side of the transformer (25 V/div)(d) Current through the primary side of the transformer (6 A/div)(e) Voltage across the secondary side of the transformer (100 V/div) (f) Output voltage (100 V/div) and output current (1 A/div)

Table 3 PI Parameters Obtained from Optimization algorithm

Input Voltage	Controller	K_{p1}	K_{i1}	K_{p2}	K_{i2}	Gain Margin	Phase Margin	Gain Cross Over frequency	Bandwidth Deviation
Case (i)	PI Controller [17]	1.6	5526.4	102.81	8812.256	inf	59.8^0	125	
V_d = 22 V, R_L = 400 Ω	ABC-tuned PI Controller	2.3336	5993.4	75.2087	8500	inf	48.7°	109	16 rad/sec
Case (ii)	PI Controller [17]	1.6	5526.4	102.81	8812.256	inf	59.2°	125	
V_d = 40 V, R_L = 400 Ω	ABC-tuned PI Controller	2.4745	5898.8	75	8504.2	inf	48.6°	109	16 rad/sec
Case (iii)	PI Controller [17]	1.6	5526.4	102.81	8812.256	inf	59°	125	
V_d = 22 V, R_L = 450 Ω	ABC-tuned PI Controller	2.3489	5972.9	105.8859	9000	inf	52.9°	123	2 rad/sec
Case (iv)	PI Controller [17]	1.6	5526.4	102.81	8812.256	inf	59.4°	125	
V_d = 40 V, R_L = 450 Ω	ABC-tuned PI Controller	2.4240	5980.4	104.7471	8904.3	inf	59.7	126	1 rad/sec
Case (v)	PI Controller [17]	1.6	5526.4	102.81	8812.256	inf	58.7°	125	
V_d = 27 V, R_L = 500 Ω	ABC-tuned PI Controller	2.1847	5916	145.3299	8500	inf	71.9°	156	31 rad/sec
Case (vi)	PI Controller [17]	1.6	5526.4	102.81	8812.256	inf	58.8°	125	
V_d = 40 V, R_L = 500 Ω	ABC-tuned PI Controller	2.2084	6000	149.9999	8500	inf	72.9°	160	35 rad/sec

7. Conclusion

The ABC-tuned PI control algorithm used for real-time implementation of DC–DC converter has high noise rejection and immunity toward external noise. From the experimental results for different input voltage and load conditions, it can be observed that the overshoot (or) undershoot in output voltage is around 0.3%. The output voltage is maintained constant with sudden change in load condition and for nonlinear loads. It demonstrates the stable performance of the controller over wide input voltage and different load conditions. During the transient period, the output voltage remains unaffected. Therefore, the switches do not experience any temporary voltage spike ensuring safe operation of switches. The controller is designed considering converter characteristics and holds good for real-time applications. Controller makes sure that the system is stable and regulates the output voltage and power with high performance and safe operation.

Appendix A

This appendix is provided to present the numerator and denominator coefficients of control-to-output voltage transfer functions of the proposed converter without PI controller

$$a_0 = \frac{2LCI_dV_c}{V_0}$$

$$a_1 = \frac{2C_0}{n}(1-D+D'')c_1 + \frac{4I_dL(1-D)}{V_0}c_2 + \frac{(1-D)^2L}{f_sL_k}c_3$$

$$a_2 = 2(1-D)^2\left[\frac{(1-D+D'')}{nf_sL_k} + \frac{2I_d}{V_0}\right]c_1 - \frac{4(1-D)(1-D+D'')}{n}c_2 + 4(1-D)^2c_3$$

$$b_0 = LCC_0$$

$$b_1 = \frac{(1-D)^2C_0L}{f_sL_k} + LC\left[\frac{1}{R_L} + \frac{2I_d}{nV_0}(1-D+D'')\right]$$

$$b_2 = \frac{(1-D)^2L}{f_sL_k}\left(\frac{1}{R_L} + \frac{2I_d}{nV_0}(1-D+D'')\right) + 4(1-D)^2C_0$$

$$b_3 = 4(1-D)^2\left[\frac{1}{R_L} + \frac{2I_d}{nV_0}(1-D+D'') + \frac{(1-D)}{n^2f_sL_k}(1-D+D'')\right]$$

$$c_1 = 2V_c$$

$$c_2 = 2\left[\frac{T_s(1-D)}{L_k}\left(V_c - V_0/n\right) - I_d\right]$$

$$c_3 = -\frac{2I_dV_c}{V_0}$$

Appendix B

This appendix is provided to present the numerator and denominator coefficients of inductor current to the duty ratio of transfer function

$$a_0 = 2V_cC_0C$$

$$a_1 = \frac{2V_cC_0(1-D)^2}{f_sL_k} + 2V_cC\left(\frac{1}{R_L} + \frac{2I_d}{nV_0}(1-D+D'')\right) + \frac{2(1-D)^3C_0}{f_sL_k}$$

$$a_2 = \frac{2(1-D)^2}{f_sL_k}\left(\frac{1}{R_L} + \frac{2I_d}{nV_0}(1-D+D'')\right)(V_c+1-D) + \frac{4I_d(1-D)^4}{nf_sL_kV_0}$$

References

[1] Y. Lembeye, V.D. Bang, G. Lefevre, and J.P Ferrieux, "Novel half-bridge inductive dc–dc isolated converters for fuel cell applications", *IEEE Trans, Energy Convers* , vol. 24, no.1, pp. 203-210, Mar. 2009.

[2] M. Nyman and M.A.E Anderson, "High-efficiency isolated boost dc–dc converter for high-power low-voltage fuel cell applications", *IEEE Trans. Ind. Electron.*, vol. 57, no.2, pp. 505-514, Feb. 2010.

[3] Y. Lembeye, V.D. Bang, G. Lefevre, and J.P. Ferrieux, " Novel half-bridge inductive dc–dc isolated converters for fuel cell applications", *IEEE Trans. Energy Convers.*, vol. 24, no.1, pp. 203-210, Mar. 2009.

[4] A.K. Rathore, A.K.S ,Bhat, and Oruganti, " Analysis and design of active-clamped ZVS current-fed dc–dc converter for fuel cells to utility interface application", *in Proc. IEEE Int. Conf. Ind. Syst*., 2007, pp. 503-508.

[5]K. Jin and X. Ruan, "Hybrid full-bridge three-level LLC resonant converter – A Novel dc–dc converter suitable for fuel-cell power system", *IEEE Trans. Ind. Electron*., vol. 53, no.5, pp.1492-1503, Oct. 2006.

[6] M. Kheirmand, M. Mahdavian, M. B. Poudeh, and S. Eshtehardiha, "Intelligent modem controller on dc–dc converter", *in Proc. IEEE Region 10 Conf.*, 2008, pp. 1-5.

[7] K. Wei, Q. Sun, B. Liang, and M. Du, "The research of adaptive fuzzy PID control algorithm based on LQR approach in DC–DC converter*", in Proc. Computational Intelligence Conf.*, vol. 1, 2008, pp. 139-143.

[8] D. Karaboga, "An idea based on honey bee swarm for numerical optimization", Technical Report – TR06, Erciyes University, Engineering Faculty, Computer Engineering Department, 2005.

[9] D. Karboga and B. Akay, "A comparative study of artificial bee colony algorithm", *Applied Mathematics and Computation*, vol. 214.2009, pp.108-132.

[10] Y. Sonmez, "Estimation of fuel cost curve parameters for thermal power plants using ABC", *Turkish Journal of Electrical Engineering and Computer Science*, vol. 21, pp. 1827-1841, 2013.

[11] N. Albert Singh, K. A. Muraleedharan, K. Gomathy, " Damping of low frequency oscillations in power system network using swarm intelligence tuned fuzzy controller", *Int. J. Bio-Inspired Computation*, vol. 2, no.1, pp. 1-8, 2010.

[12] Zwe-Lee Gaing, "A Particle Swarm Optimization approach for optimum design of PID controller in AVR system", *IEEE. Trans. Energy conversion* , vol. 19, no. 2, pp. 384-391, June 2004.

[13] R. A. Krohling and J. P. Rey, "Design of Optimal disturbance rejection PID controllers using genetic algorithm", *IEEE Trans. Evol. Comput*., vol. 5, pp. 78-82. Feb. 2001.

[14] Eajal A. El-Hawary ME. Optimal capacitor placement and sizing in unbalanced distribution systems with harmonics consideration using Particle Swarm Optimization", *IEEE Trans. Power Deliv* , vol. 25, no. 3, pp. 1734-1741, July 2010.

[15] Szuvovivski I Fernandes TSP, Aoki AR. "Simultaneous allocation of capacitors and voltage regulators at distribution networks using Genetic Algorithms and Optimal Power Flow", *Electric Power Energy Syst.* vol. 40, pp. 62-69, 2012.

[16] H. Yoshida, K. Kawata and Y. Fukuyama, "A Particle Swarm Optimization for reactive power and voltage control considering voltage security assessment", *IEEE Trans. Power Syst*., vol. 15, pp. 1232-1239, Nov. 2000.

[17] Udupi R Prasanna, Akshay K. Rathore, " Small – Signal Modeling of Active – Clamped ZVS Current – Fed Full – Bridge Isolated dc–dc Converter and Control

System Implementation using PSOC. ", *IEEE Trans. Ind. Electron*., vol.61, no.3, pp. 1253-1261, Mar. 2014
[18] Sheng Zong, HaozeLuo, WuhuaLiandChangliang Xia, "Theoretical Evaluation of Stability Improvement brought by resonant current loop for Paralleled LLC Converters", *IEEE trans, Ind Electron, in press.*
[19] FonkeweFongang Edwin, Weidong Xiao, VinodKhadkikar, " Dynamic Modeling and Control of Interleaved Flyback Module-Integrated Converter for PV Power Applications", *IEEE trans, Ind Electron*, vol. 61, no. 3, Mar. 2014.
[20] S. Zengin, F. Deveci and M. Boztepe, "Decoupling capacitor selection in DCM flyback PV microinverters considering harmonic distortion", *IEEE Trans. Power Electron*., vol .28, no.2 , pp. 816-825, Feb.2013.
[21] R. Venkatraman and A.K.S Bhat, "Small-signal analysis of a soft switching, single-stage two-switch ac-to-dc converter", *in Proc, IEEE Power Electron, Spec , Conf* ., 2001, pp. 1824-1830.